THE JOURNAL OF PHYSICAL CHEMISTRY C

Article

pubs.acs.org/JPCC

Photovoltaic Efficiency Enhancement of Cu_2O Solar Cells Achieved by Controlling Homojunction Orientation and Surface Microstructure

H. M. Wei, H. B. Gong, L. Chen, M. Zi, and B. Q. Cao*

Key Laboratory of Inorganic Functional Materials in Universities of Shandong, School of Material Science and Engineering, University of Jinan, Jinan, 250022, China

ABSTRACT: Controlling the interface quality and surface microstructure of the cuprous oxide (Cu_2O) p−n homojunction is crucial to obtaining high-efficiency film solar cells. However, the low-cost synthetic techniques for preparing such homojunction structures with a high-quality interface and designed surface microstructure still remain a challenge because of the doping difficulty for the n-type of Cu_2O, especially with aqueous precursors. Herein, we report an electrochemical deposition approach to growing the Cu_2O p−n homojunction by selecting proper electrolytes of different pH levels. The Cu_2O film growth orientation and surface microstructure are controlled by adjusting the applied deposition potential and the precursor concentration. The epitaxial growth of the Cu_2O homojunction with n/p films of the same crystal orientation reduces the interface states and the formation of a textured structure on the surface helps the photons to be absorbed more effectively, which both enhance the photovoltaic conversion efficiency of Cu_2O film solar cells. Our findings provide an effective method for the fabrication of Cu_2O homojunctions with a high-quality interface and textured surface, which can pave the way to further improve the photovoltaic properties of Cu_2O-based film solar cell devices.

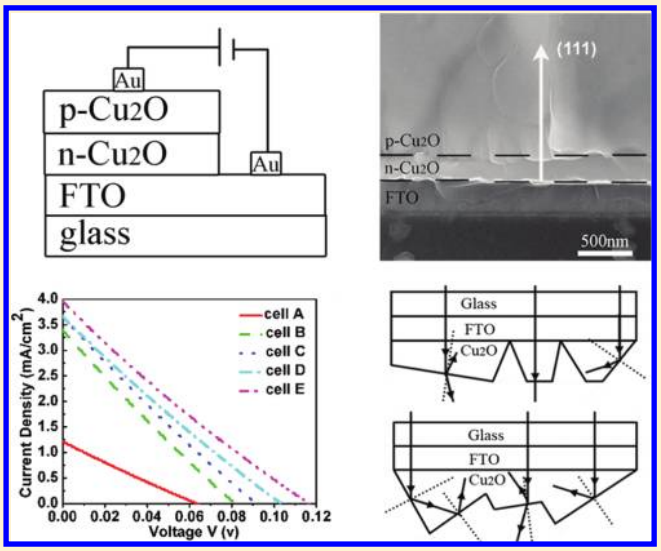

1. INTRODUCTION

Cuprous oxide (Cu_2O) is a very promising material for the fabrication of solar cells due to the direct band gap (1.9−2.2 eV) and relatively high absorption coefficient in the visible region.[1−4] It also has many interesting characteristics, such as low production cost, nontoxicity, and fairly high minority carrier diffusion length. Theoretical calculations have predicted a photovoltaic conversion efficiency of approximately 19%.[5] Different kinds of Cu_2O-based solar cells have been fabricated with metal/p-Cu_2O Schottky junctions[6] and p−n heterojunctions, such as n-ZnO/p-Cu_2O,[7,8] n-CdO/p-Cu_2O,[9] or n-$Sn_{1-x}Co_xO_2$/p-Cu_2O.[10] The efficiencies of the above solar cells were usually smaller than 1%. Recently, Mittiga et al.[11] reported the fabrication of heterojunction solar cells made by deposition of transparent conducting oxide films on Cu_2O substrates, and the best solar cell reached a conversion efficiency of 2%. This is the highest efficiency obtained up to now with a p−n heterojunction, which is still much lower than the theoretical efficiency limit of the Cu_2O solar cell. The above low efficiency can be mainly attributed to the lack of p−n homojunctions due to the difficulty to find a proper technique of doping Cu_2O to get low-resistivity n-type semiconductors.

Although it is well believed that the best way to improve the photovoltaic efficiency of Cu_2O-based solar cells is to achieve a PN homojunction with both n-type and p-type Cu_2O materials, only a handful of experimental methods to prepare n-type Cu_2O have been reported to date.[12] Siripala et al.[13] reported that the electrodeposited Cu_2O films behave as an n-type semiconductor material when used as a liquid/solid junction in a photoelectrochemical cell in 1996. Fernando et al.[14] and Jayewardena et al.[15] then reported a similar synthesis method of boiling copper plates in $CuSO_4$ or HCl solution to prepare Cu_2O film, and both observed an n-type signal from a photoelectrochemical cell. In 2007, Wang et al.[16] grew n-type Cu_2O by electrochemical deposition and observed n-type conductivity through Mott−Schottky capacitance−voltage measurements. McShane et al.[17] observed obvious photocurrent enhancement of n-type Cu_2O films by controlling the dendritic branching electrochemical deposition growth. Han et al.[18] fabricated Cu_2O homojunction Cu_2O solar cells by electrochemical deposition and optimized the film resistivity with a result of a photovoltaic conversion efficiency of 0.1%. More recently, the effect of junction morphology on the performance of polycrystalline Cu_2O film solar cells was also studied.[19]

Received: February 27, 2012
Revised: April 8, 2012
Published: April 10, 2012

However, in most of the previous investigations of Cu_2O thin film growth, film orientation and microstructure were not well-controlled. The lack of high-quality homojunction interfaces between n-type Cu_2O and p-type Cu_2O reduces the open-circuit voltage and fill factor and results in low photovoltaic efficiency. Therefore, more intensive study is necessary. In this paper, we investigated the controlled growth of Cu_2O by electrochemical deposition in order to better understand and control the homojunction properties. An effective way to increase the Cu_2O solar cell efficiency by tuning the homojunction interface crystal orientation and forming a pyramid-like textured surface was reported. They were both realized by optimizing the electrochemical growth conditions, which is a simple, efficient, and low-cost method.

2. EXPERIMENTAL SECTION

2.1. Growth of Cu_2O Films. All the used chemicals were bought from Sinopharm Chemical Reagent Company Limited (Shanghai, China), and the FTO glass (TEM C15) was bought from Nippon Sheet Glass (NSG) Group (Tokyo, Japan). The conductive glass slides coated with layers of 350 nm fluorine-doped tin oxide (FTO glass) were used as the cathodes (~1 cm^2). The square resistance is about 14 Ω/sq. Galvanostatic cathode deposition of Cu_2O films was performed in a standard three-electrode electrochemical cell. Graphite sheets acted as the anode, and the Ag/AgCl reference electrode was used. p-type Cu_2O films were electrodeposited at 60 °C with a pH value of 11 adjusted by adding some NaOH solution. Two electrolytes were adopted, one was Solution (I), containing copper sulfate (0.02 M) and lactic acid (0.4 M), and the other was Solution (II), containing copper sulfate (0.4 M) and lactic acid (5 M). The applied potential was −0.2 V, and the deposition time was 60 min.

n-type Cu_2O films could be grown by electrochemical deposition in acid solution according to the former reports.[14−19] In this study, an aqueous solution containing 0.02 M copper acetate and 0.08 M acetic acid was used as the electrolyte with a pH value of 4.9 adjusted by adding some NaOH solution. The deposition potential was between −0.03 and −0.2 V. The deposition temperature was fixed at 60 °C by a water bath, and the deposition time was 60 min for all samples. For the growth of different Cu_2O homojunctions, n-type Cu_2O films were first electrodeposited on FTO glass substrates, which were then used as cathodes for subsequent p-type film growth. Finally, Cu_2O homojunctions were ready for characterizations and device fabrications. Experimental conditions are listed in Table 1.

Table 1. Electrochemical Deposition Growth Conditions of Five Typical Cu_2O p−n Homojunction Solar Cells Together with the Film Orientations and Surface Microstructures

	n-Cu_2O pH: 4.9, Cu^{2+} concentration (mol L^{-1}): 0.05		p-Cu_2O pH: 11, deposition potential (V): −0.2	
solar cell	applied potential (V)	orientation	Cu^{2+} concentration (mol L^{-1})	surface microstructure
A	−0.20	⟨200⟩	0.02	⟨111⟩
B	−0.10	⟨200⟩	0.02	⟨111⟩
C	−0.05	⟨200⟩	0.02	⟨111⟩
D	−0.03	⟨111⟩	0.02	⟨111⟩
E	−0.03	⟨111⟩	0.40	⟨111⟩, texture

2.2. Materials and Device Characterizations. Morphological characterizations of Cu_2O films and homojunction structures were performed with an FEI Quanta scanning electron microscope (SEM). X-ray diffraction (XRD) (D8-Advance, Bruker) was used to examine the crystal structure and orientation of the films. A cool sputter coater (SCD 005, Bal-Tec) with designed masks was applied to deposit gold contacts on samples and FTO glasses. Photovoltaic measurements were recorded employing a 3A solar simulator (XES-40S1, San-Ei) with an AM 1.5 spectrum distribution. The power of the light was calibrated against an ISE CalLab Fraunhofer silicon reference cell to simulate one full sun intensity (100 mW/cm^2). The solar cells were fixed on a temperature-controlled sample test stage (0821, Vision-Tec) to keep the devices at a temperature of 25 °C and were illuminated from the glass substrate side. The current−voltage (I−V) characteristics of the fabricated Cu_2O solar cells were measured with a Keithley 2612A source/meter.

3. RESULTS AND DISCUSSIONS

Figure 1a,b shows the typical surface morphology of p-type Cu_2O film electrodeposited with different concentrations of copper sulfate solution, but at the same deposition potential of −0.2 V. Under the same deposition potential, the particle size of the film decreases with the increase of concentration of electrolyte. It can be easily understood that it was due to the increase of nucleation density under higher electrolyte concentration. Careful observations of the SEM images found that the film surface, composed of tilted {100} faces, exhibits 3-fold rotational axes at the center of triangular faces and 3-fold axes at the apexes. Therefore, the surface of the p-type Cu_2O film shows a pyramid-like morphology, especially in Figure 1b, which is similar to the textured surface structure of crystalline silicon solar cells.[20−24] The pyramid-like surface microstructure was formed by a higher growth ratio (R ~ 1.7) along the ⟨100⟩

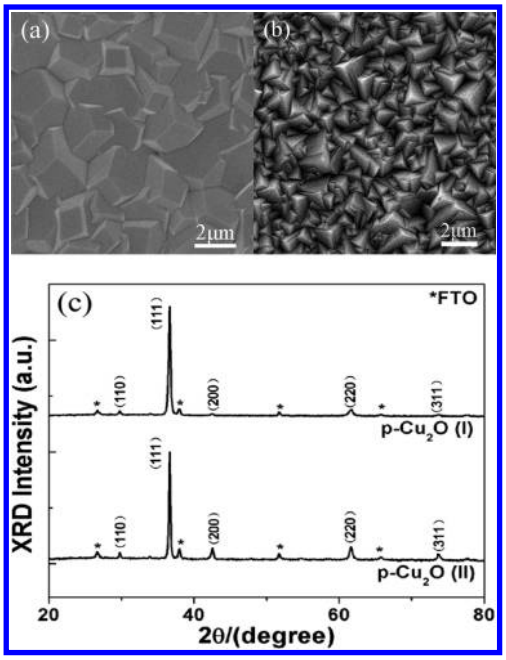

Figure 1. Top-view SEM images of the p-type Cu_2O layers obtained by (a) Solution I and (b) Solution II. (c) Corresponding XRD patterns of Cu_2O films shown in (a) and (b), respectively.

dx.doi.org/10.1021/jp301904s | J. Phys. Chem. C 2012, 116, 10510−10515

direction to that along the ⟨111⟩ direction when the electrolyte concentration was higher.[25]

Figure 1c displays their XRD patterns of the Cu_2O layers accordingly. Besides the diffraction peak with asterisks from the FTO conductive film on glass, all other diffraction peaks can be identified as the standard cubic cuprous oxide (PDF no. 050667). With a powder XRD Bragg–Brentano geometry, only the reflections from the crystallographic planes parallel to the substrate can be collected. Therefore, the relative intensities of different reflection peaks provide information regarding the crystal orientation against the substrate. Considering that the calculated diffraction intensity ratio of the (111) peak to the (200) peak is 2.7 for Cu_2O powders, the XRD of Figure 1c indicates that the films are dominantly of [111]-preferred orientation for both films deposited in Solution (I) and Solution (II). It is worth mentioning that, in our serial experiments, the growth of CuO is much more difficult than that of Cu_2O film, although both of them can be obtained with ECD depending on the growth conditions.[26] However, after annealing at 400 °C for 1 h, the ECD grown Cu_2O can change to CuO totally or partially (XRD data not shown here).[27,28]

Figure 2 shows the typical surface morphologies of the Cu_2O layers electrodeposited with 0.02 M copper acetate solution at a

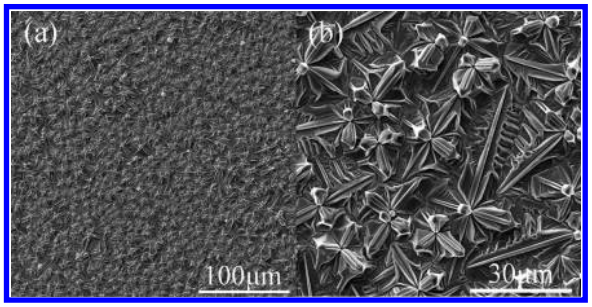

Figure 2. Top-view SEM image of the n-type Cu_2O layer. Panel (a) shows the surface morphology on a large scale and (b) displays the typical dendritic growth behavior.

pH value of 4.9, which was similar to the reported high-performance n-type Cu_2O photoelectrodes.[17] The n-type Cu_2O layers exhibit typical dendritic branching growth behavior caused by acetate buffer, which is also a morphology characteristic of n-type Cu_2O layers grown with the electrochemical method.[29,30] The partial enlargement of Figure 2b shows that the Cu_2O crystal branches grown on the substrate are significantly longer than the branches grown out of the substrate. This was mainly due to that the FTO glass is much more conductive than the semiconductive Cu_2O, resulting in the electrodeposition on the conductive substrate being faster than the growth out of the substrate. From the viewpoint of film solar cell fabrication, such a dendritic crystal growth is highly desirable as it is easy to cover the whole substrate.

To determine the preferred orientation of the n-type Cu_2O layers electrodeposited from −0.03 to −0.2 V, XRD measurements were performed. Although the surface morphology of Cu_2O film does not show a clear change with deposition potential, the relative intensities of XRD peaks change obviously, as shown in Figure 3. It indicates that the growth orientation of n-type Cu_2O layers is dependent on the deposition potential. The XRD peak intensity ratio of $I(111)/I(200)$ ($R111/200$) for the two most strong peaks is plotted as a function of the deposition potential, as shown in

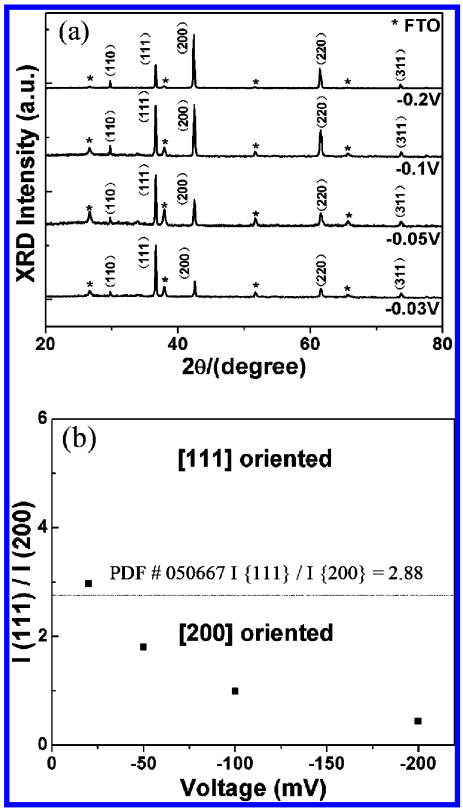

Figure 3. (a) XRD patterns of n-Cu_2O electrodeposited under different potentials. (b) Plot of relative peak intensity of $I(111)/I(200)$ as a function of deposition potential.

Figure 3b. For ordinary Cu_2O powders with a random orientation, the intensity ratio of $R111/200$ is 2.7. If this ratio is bigger than 2.7, n-type Cu_2O film is of [111]-preferred crystal orientation, whereas the sample exhibits a [100] orientation.[31,32] The n-type Cu_2O electrodeposited at potential of −0.03 V is of [111]-preferred orientation as the $R111/200$ value is bigger than 2.7. With the electrodeposited potential increasing more negatively, the $R111/200$ value decreases and becomes smaller than 2.7, indicating that such layers gradually exhibit a [100]-preferred orientation. On the basis of this, the Cu_2O homojunction with the same growth orientation could be obtained by tuning the n-type and p-type films' orientation, respectively.

On the basis of the above surface morphology and growth orientation control results, five Cu_2O p–n homojunction solar cells were fabricated, and the growth conditions are summarized in Table 1. Their typical film orientation and surface microstructure were also compared. The final device structure is schematically illustrated in Figure 4a. Figure 4b shows a typical cross-sectional SEM image of solar cell D, where a homojunction constructed with 230 nm n-type and 4 μm p-type Cu_2O layers can be observed.

The dark current density–voltage (I–V) characteristics of different solar cells are shown in Figure 4c. With the applied electrodeposition potential decreasing from cell A to cell D, the reverse current density under the same bias reduced clearly. With −2 V applied bias, the reverse current density of cell A is 0.23 mA/cm^2, whereas it is 0.05 mA/cm^2 for cell D. As cell A is composed of p/n Cu_2O layers of different orientations and cell D is composed of Cu_2O layers of both ⟨111⟩ orientations, the reverse current reduction can be mainly attributed to the

dx.doi.org/10.1021/jp301904s | J. Phys. Chem. C 2012, 116, 10510–10515

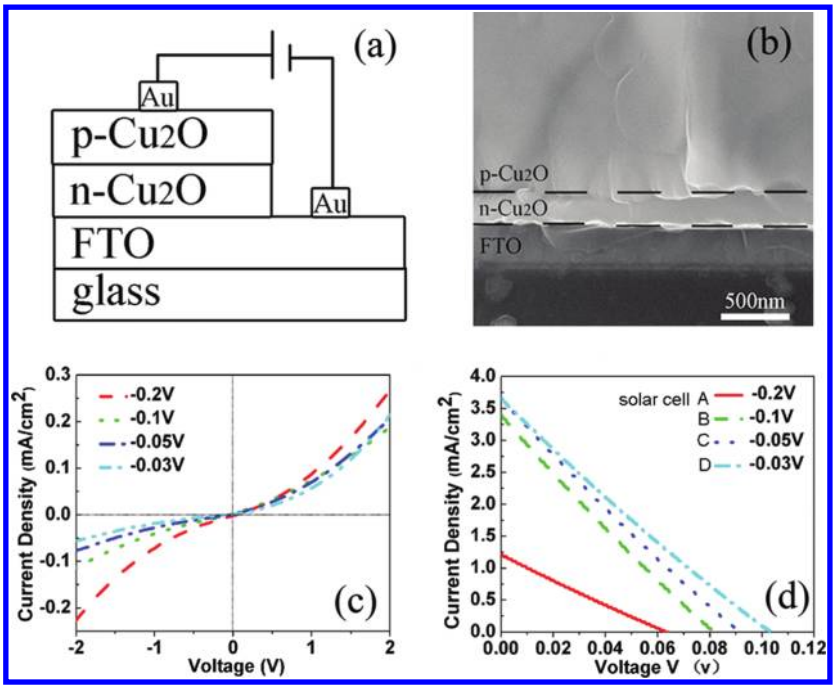

Figure 4. (a) Structural scheme of the Cu_2O homojunction solar cell. (b) Side-view SEM image of the Cu_2O homojunction. (c) Dark $I-V$ characteristics of the Cu_2O homojunction. (d) Current−voltage ($I-V$) characteristic curves of the Cu_2O homojunction solar cells obtained by different deposition potentials.

seamless epitaxial growth of p-type onto n-type Cu_2O layers when their growth orientation was consistent. In this case, the crystal lattice could maintain continuity and reduce the interface states and form a high-quality interface with a result of reverse current reduction.[19]

The $I-V$ characteristic curves under an AM 1.5 solar simulator irradiation of 100 mW/cm^2 and the corresponding calculated characteristic parameters of different cells are shown in Figure 4d and Table 2, respectively. The cell A fabricated

Table 2. Photovoltaic Properties of the Cu_2O Homojunction Solar Cells (A−E) with Different Film Orientations and Surface Microstructures

solar cell	V_{oc} (V)	J_{sc} (mA cm^{-2})	FF (%)	PCE (%)
A	0.06	1.40	24.1	0.021
B	0.08	3.40	23.6	0.065
C	0.09	3.65	23.5	0.078
D	0.10	3.66	23.3	0.088
E	0.12	3.97	22.6	0.104

with a ⟨111⟩-orientated p-type Cu_2O onto a ⟨100⟩-orientated n-type layer shows an open-circuit voltage (V_{OC}) of 0.06 V, a short-circuit density (J_{SC}) of 1.4 mA/cm^2, a fill factor (FF) of 24.1%, and a photovoltaic conversion efficiency (PCE) of 0.021%. With the reduction of deposition potential, all the V_{OC}, J_{SC}, and PCE increased obviously. The cell D composed of Cu_2O layers of the same orientations exhibits higher V_{OC}, J_{SC}, and PCE of 0.10 V, 3.66 mA/cm^2, and 0.088%, respectively, which further confirm the formation of a p−n homojunction with higher quality.

Figure 5a further compares the $I-V$ characteristic curves of cell D and cell E, which have different surface microstructures of p-type Cu_2O layers. As shown in Figure 1b, a pyramid-like surface morphology was obtained when a high concentration solution of copper sulfate and lactic acid was used to grow the

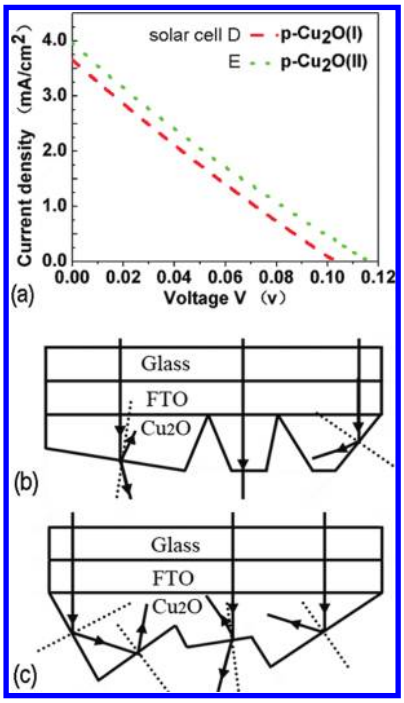

Figure 5. (a) Current−voltage ($I-V$) characteristic curves of the Cu_2O homojunction solar cells with different surface microstructures under one full sun illumination. (b, c) Light propagation pathway through Cu_2O homojunction solar cells corresponding to cells D and E, respectively.

p-type Cu_2O layer. Figure 5b,c schematically illustrates the structure of cell D and cell E. Interestingly, the photovoltaic performance of cell E was further improved in comparison with that of cell D with V_{OC}, J_{SC}, and PCE of 0.12 V, 3.97 mA/cm^2, and 0.104%, respectively, as listed in Table 2.

dx.doi.org/10.1021/jp301904s | J. Phys. Chem. C 2012, 116, 10510−10515

4. DISCUSSION

4.1. Influences of Crystal Orientations. According to the Shockley p−n junction model and the known data of Cu_2O electron affinity (3.2 eV) and band gap (2.1 eV), Figure 6a shows the proposed energy band diagram for the Cu_2O homojunction. When the homojunction is formed, electrons diffuse from the n-type side, which has a higher Fermi level, to the p-type side, as it is abundant in n-type material. The similar process happens for holes in the p-type Cu_2O layer. As a result, the unified Fermi level will form and the flow of charges sets up a built-in electrical field. The built-in potential depends on the Fermi level difference between n-type and p-type film, and the V_{OC} of the Cu_2O solar cell can be estimated with $V_{OC} \approx V_p + V_n$,[33] which can also be influenced by interface states of a homojunction. Interface states introduce a mass of defect levels and change the work function at the interface. The photoelectrons will be captured by interface states and recombined with holes. As a result, the interface states offset the effect of the built-in potential through the energy band bending, as shown in Figure 6b, and lead to the open-circuit voltage reduction.[34] By tuning the n-Cu_2O film growth orientation from ⟨100⟩ to ⟨111⟩ to match the p-Cu_2O orientation, the formation of interface states during the homojunction epitaxial growth can be restrained, which can effectively prevent recombination of electrons in n-Cu_2O with holes in p-Cu_2O at the interface region and enhance the built-in potential. Therefore, the V_{OC} increase from cell A to cell D is mainly due to the interface quality enhancement by controlling the film growth orientation. However, the V_{OC} is still lower than the best reported value of ~0.4 V.[19] One possible reason is that such Cu_2O films prepared by electrochemical deposition are of a low doping level, especially for n-type films, and only a weak built-in electrical field is formed. The increase of J_{SC} is also due to the seamless epitaxial growth of p-Cu_2O onto n-Cu_2O with the same crystal orientations that reduces the leakage current caused by interface states. Therefore, the photovoltaic performance from cell A to cell D is enhanced, as shown in Table 2.

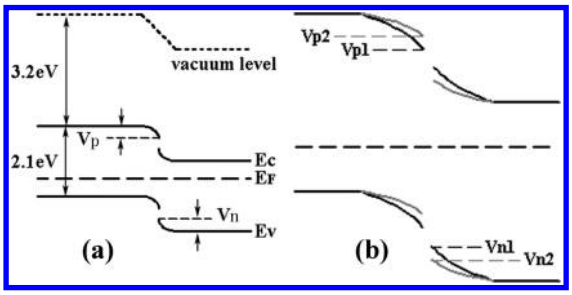

Figure 6. (a) Proposed energy band diagram for the Cu_2O p−n homojunction. (b) Schematic diagram of energy band bending influence by interface states.

4.2. Influence of Surface Microstructure. The influence of the surface microstructure of p-type Cu_2O layers on the photovoltaic properties is mainly due to the different light propagation pathway in the Cu_2O solar cells. When the light passes through the FTO glass substrate and solar cell, the unabsorbed light will arrive at the Cu_2O/air interface. Both reflection and refraction can happen here. As the refraction index of Cu_2O (2.7) is bigger than that of air, total internal reflection will happen if the incidence angle is greater than the critical angle (21°). In comparison with cell D, the pyramid-like surface texture of cell E is composed of more tilted (111) planes relative to the top horizontal glass surface. This would result in more light reflected back to the solar cell at the Cu_2O/air interface by total internal reflection, as compared in Figure 5b,c. This means that the pyramid-like surface structure of p-Cu_2O caused the increase of the light path in the solar cell that could facilitate the photons to be absorbed more effectively. Therefore, the short-circuit current density of cell E increased, as shown in Figure 5a. The small pyramid-like particles in p-type Cu_2O of cell E were also beneficial to depositing the following n-type layer and forming a continuous p−n homojunction with higher interface quality. This resulted in the efficient transfer of photoexcited charges and increases the V_{OC} of cell E in comparison with that of cell D.

Finally, it should be pointed out that the Cu_2O films with varied orientations grown under different ECD conditions would have different electrical properties, which also has an influence on the performance of solar cells. Therefore, their electrical properties, such as carrier concentration and sheet resistance, should be measured, for example, Hall measurements. However, such Cu_2O film grown on an FTO glass substrate is much more conductive than the semiconductive Cu_2O. This makes electrical measurements difficult. In the future, other characterization methods should be found out to study the electrical properties of different Cu_2O layers to clarify their influence on the solar cell properties.

5. CONCLUSIONS

In summary, p/n-type Cu_2O films were fabricated with electrochemical deposition by selecting different electrolytes and optimizing pH levels. The growth orientation of n-Cu_2O films can be tuned from ⟨100⟩ to ⟨111⟩ by decreasing the applied deposition potential. Therefore, the epitaxial growth of p-Cu_2O film onto n-film with the same ⟨111⟩ orientation facilities the formation of a homojunction with a high-quality interface by reducing interface states. A pyramid-like surface texture structure was realized by selecting the proper concentration of electrolytes, which helped the photons to be absorbed more effectively by increasing the light path. The improvement of the interface quality of the p−n junction and the formation of surface texture both enhance the photovoltaic conversion efficiency of Cu_2O film solar cells. The successful growth of high-quality Cu_2O homojunctions with a designed surface structure via a controllable and low-cost solution deposition method by optimizing electrochemical conditions opens up a new way to improve the photovoltaic performance of Cu_2O-based devices.

■ AUTHOR INFORMATION

Corresponding Author

*E-mail: mse_caobq@ujn.edu.cn.

Notes

The authors declare no competing financial interest.

■ ACKNOWLEDGMENTS

This work is supported by the NSFC (51002065, 11174112) and the Shandong Provincial Science Foundation for Distinguished Youth Scholars (2012JQB01031; BS2010CL003). B.Q.C. thanks the Taishan Scholar Professorship (TSHW20091007) tenured at University of Jinan. The Program for New Century Excellent Talents in University (NCET-11-1027) and the Research Foundation for Returned

Oversea Students, Ministry of Education, China, are also acknowledged.

REFERENCES

(1) Olsen, L. C.; Bohara, R. C.; Urie, M. W. *Appl. Phys. Lett.* **1979**, *34*, 47−49.
(2) Rakhshani, A. E. *Solid-State Electron.* **1986**, *29*, 7−17.
(3) Ma, L. L.; Lin, Y. L.; Wang, Y.; Li, J. L.; Wang, E.; Qiu, M. Q.; Yu, Y. *J. Phys. Chem. C* **2008**, *112*, 18916−18922.
(4) Shi, H.; Yu, K.; Sun, F.; Zhu, Z. Q. *CrystEngComm.* **2012**, *14*, 278−285.
(5) Henry, C. H. *J. Appl. Phys.* **1980**, *51*, 4494−4500.
(6) Iwanoski, R. J.; Trivich, D. *Sol. Cells* **1984**, *13*, 253−264.
(7) Wei, H. M.; Gong, H. B.; Wang, Y. Z.; Hu, X. L.; Chen, L.; Xu, H. Y.; Liu, P.; Cao, B. Q. *CrystEngComm* **2011**, *13*, 6065−6070.
(8) Cui, J. B. *J. Phys. Chem. C* **2010**, *114*, 6408−6412.
(9) Papadimitriou, L.; Economou, N. A.; Trivich, D. *Sol. Cells* **1981**, *3*, 73.
(10) Shiu, H. Y.; Tsai, C. M.; Chen, S. Y.; Yew, T. R. *J. Mater. Chem.* **2011**, *21*, 17646−17650.
(11) Mittiga, A.; Salza, E.; Sarto, F.; Tucci, M.; Vasanthi, R. *Appl. Phys. Lett.* **2006**, *88*, 163502.
(12) Garuthara, R.; Siripala, W. *J. Lumin.* **2006**, *121*, 173−178.
(13) Siripala, W.; Perera, L. D. R. D.; Silva, K. T. L. D.; Jayanetti, J. K. D. S.; Dharmadasa, I. M. *Sol. Energy Mater. Sol. Cells* **1996**, *44*, 251−260.
(14) Fernando, C. A. N.; Wetthasinghe, S. K. *Sol. Energy Mater. Sol. Cells* **2000**, *63*, 299−308.
(15) Jayewardena, C.; Hewaparakrama, K. P.; Wijewardena, D. L. A.; Guruge, H. *Sol. Energy Mater. Sol. Cells* **1998**, *56*, 29−33.
(16) Wang, L. C.; Tao, M. *Electrochem. Solid-State Lett.* **2007**, *10*, H248−H250.
(17) McShane, C. M.; Choi, K. -S. *J. Am. Chem. Soc.* **2009**, *131*, 2561−2569.
(18) Han, K.; Tao, M. *Sol. Energy Mater. Sol. Cells* **2009**, *93*, 153−157.
(19) McShane, C. M.; Siripala, W. P.; Choi, K.-S. *J. Phys. Chem. Lett.* **2010**, *1*, 2666−2670.
(20) Nishimoto, Y.; Namba, K. *Sol. Energy Mater. Sol. Cells* **2000**, *61*, 393−402.
(21) Iencinella, D.; Centurioni, E.; Rizzoli, R.; Zignani, F. *Sol. Energy Mater. Sol. Cells* **2005**, *87*, 725−732.
(22) Papet, P.; Nichiporuk, O.; Kaminski, A.; Rozier, Y.; Kraiem, J.; Lelievre, J.-F.; Chaumartin, A.; Fave, A.; Lemiti, M. *Sol. Energy Mater. Sol. Cells* **2006**, *90*, 2319−2328.
(23) Gangopadhyay, U.; Kim, K.; Kandol, A.; Yi, H.; Saha, H. *Sol. Energy Mater. Sol. Cells* **2006**, *90*, 3094−3101.
(24) Vallejo, B.; González-Mañas, M.; Martínez-López, J.; Caballero, M. A. *Sol. Energy* **2007**, *81*, 565−569.
(25) Siegfried, M. J.; Choi, K.-S. *Adv. Mater.* **2004**, *16*, 1743−1746.
(26) Kothari, H. M.; Kulp, E. A.; Boonsalee, S.; Nikiforov, M. P.; Bohannan, E. W.; Poizot, P.; Nakanishi, S.; Switzer, J. A. *Chem. Mater.* **2004**, *16*, 4232−4244.
(27) Chen, L.; Shet, S.; Tang, H.; Wang, H.; Deutsch, T.; Yan, Y.; Turner, J.; Al-Jassim, M. *J. Mater. Chem.* **2010**, *20*, 6962−6967.
(28) Nair, M. T. S.; Guerrero, L.; Arenas, O. L.; Nair, P. K. *Appl. Surf. Sci.* **1999**, *150*, 143−151.
(29) Lopez, C. M.; Choi, K.-S. *Langmuir* **2006**, *22*, 10625−10629.
(30) Siegfried, M. J.; Choi, K.-S. *Angew. Chem., Int. Ed.* **2008**, *47*, 368−372.
(31) Zhou, Y. C.; Switzer, J. A. *Scr. Mater.* **1998**, *38*, 1731−1738.
(32) Bijani, S.; Martínez, L.; Gabás, M.; Dalchiele, E. A.; Ramos-Barrado, J. R. *J. Phys. Chem. C* **2009**, *113*, 19482−19487.
(33) Musselman, K. P.; Marin, A.; Wisnet, A.; Scheu, C.; MacManus-Driscoll, J. L.; Schmidt-Mende, L. *Adv. Funct. Mater.* **2011**, *21*, 573−582.
(34) Milnes, A.; Feucht, D. *Heterojunctions and Metal-Semiconductor Junctions*; Academic Press: New York, 1972.